John von Neumann Institute for Computing



Molecular Dynamics Simulations of Polyelectrolyte Brushes

Christian Seidel and N. Arun Kumar

published in

NIC Symposium 2006 ,
G. Münster, D. Wolf, M. Kremer (Editors),
John von Neumann Institute for Computing, Jülich,
NIC Series, Vol. **32**, ISBN 3-00-017351-X, pp. 253-260, 2006.

© 2006 by John von Neumann Institute for Computing
Permission to make digital or hard copies of portions of this work for personal or classroom use is granted provided that the copies are not made or distributed for profit or commercial advantage and that copies bear this notice and the full citation on the first page. To copy otherwise requires prior specific permission by the publisher mentioned above.

http://www.fz-juelich.de/nic-series/volume32

Molecular Dynamics Simulations of Polyelectrolyte Brushes

Christian Seidel and N. Arun Kumar

Max Planck Institute of Colloids and Interfaces, Theory Department
Science Park Golm, 14424 Potsdam, Germany
E-mail: {*seidel, kumar*}*@mpikg.mpg.de*

We give a short overview about molecular dynamics simulations of polyelectrolytes end-grafted to a surface. The simulation model includes counterions as well as additional salt ions explicitly and treats the full Coulomb interaction. Here we address two problems. The first one is the effect of the grafting density on the chain stretching. The second one is the effect of additional salt ions on the structure of the brush.

1 Introduction

Polyelectrolytes (PELs) are macromolecules that contain subunits having the ability to dissociate charges in polar solvents such as, e.g., water. Due to their importance in materials science, soft matter research, and molecular biology, PELs have received a lot of attention in recent years.

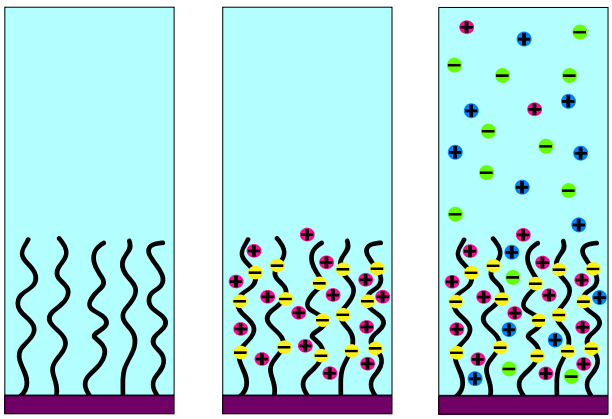


Figure 1. Schematic picture of polymer brushes. Left-hand side: made of uncharged polymers, middle: polyelectrolyte brush in the osmotic regime, right-hand side: polyelectrolyte brush with additional salt ions.

Polymer brushes consist of chains densely end-grafted to a surface. Due to various forces, tethered chains are enforced to take an elongated conformation. A schematic representation of an uncharged polymer brush is shown in Fig. 1 (left-hand part). PEL brushes form the subject of increasing interest in theory, simulation and experiment. From the application point of view, they are an effective means for, e.g., preventing colloids from flocculation.

Brushes made of charged chains have the advantage that stabilization occurs due to both steric and electrostatic effects. In addition, a surface coated with PELs is less sensitive to the salinity of the surrounding medium than a bare charged surface because a strongly charged brush is able to trap its own counterion generating a layer of high effective ion strength (Fig. 1, middle part). Nevertheless varying salt concentration is an important parameter to tune the polyelectrolyte effect and to change the structure of PELs in experiments (see Fig. 1, right-hand part). PEL brushes are also used in small devices for pH-controlled gating and are thought to be a model for the protecting envelope of cells (glycocalix).
Both in experiment and in theoretical studies, PELs are a subject with specific and unsolved problems. In such a situation, simulations are a promising tool to validate theoretical models and to probe data which are not easily accessible in experiment. However, despite strong effort in recent years, due to the long-ranged Coulomb interaction simulations of PELs remain still challenging.

2 Simulation Model and Method

The brush is represented by M freely jointed bead-spring chains of length $N+1$ which are anchored by one end to an uncharged planar surface at $z=0$. The uncharged anchor segments are fixed and form a square lattice. For completely charged chains, due to electroneutrality there are $M \times N$ monovalent counterions. Additional salt ions of monovalent 1:1 type are modeled exactly in the same way as counterions.
The chains are assumed to be in a good solvent modeled by a purely repulsive short-range interaction that is described by a shifted Lennard-Jones potential U_{LJ}. Along the chains, beads are connected by a FENE bond potential U_{bond}. With our choice of parameters we obtain an average bond length $b \approx \sigma$ where σ is the Lennard-Jones parameter. All particles except the anchor segments are exposed to a short-ranged repulsive interaction U_{wall} with the grafting surface at $z=0$. An identical wall is placed at the top boundary of the simulation box $z=L_z$. In particular the second wall is necessary to reach a finite salt concentration.
Counterions and salt ions are treated as individual, non-bonded particles and all charged entities interact with the bare Coulomb potential

$$u_{\mathrm{Coul}}(r) = k_{\mathrm{B}}T\, q_i q_j\, \frac{l_{\mathrm{B}}}{r}, \tag{1}$$

with q_i and q_j being the corresponding charges in units of elementary charge e and l_{B} is the Bjerrum length that sets the strength of the interaction. It is well known that the handling of long-range forces in simulations requires special methods[1]. To treat them in the particular $2\mathrm{D}+1$ slab geometry (the simulation box is periodic only in x and y directions while perpendicular to the grafting surface the system is restricted to one layer), now we use the so-called MMM technique introduced by Strebel and Sperb[2] and modified for laterally periodic systems $(\mathrm{MMM2D})$ by Arnold and Holm[3]. Although, due to symmetry breaking, the MMM scaling $\mathcal{O}(N_{\mathrm{tot}}\log(N_{\mathrm{tot}}))$ is not maintained in the $2\mathrm{D}+1$ case, the remaining $\mathcal{O}(N_{\mathrm{tot}}^{5/3}\log(N_{\mathrm{tot}})^2)$ behavior enables to increase significantly the total number of charged particles.
To study the system in equilibrium at constant temperature, we use stochastic molecular

dynamics where all particles are coupled to a heat bath. For using the IBM Regatta supercomputer the molecular dynamics code was parallelized by means of a self-scheduling (master-slave) algorithm[4]. We typically consider between 2 000 and 8 000 charges. Typical runtime ranges from about two to 10 days for a single data point. That is why we are forced to use supercomputers in order to be able to effectively study polyelectrolyte brushes by simulation techniques.

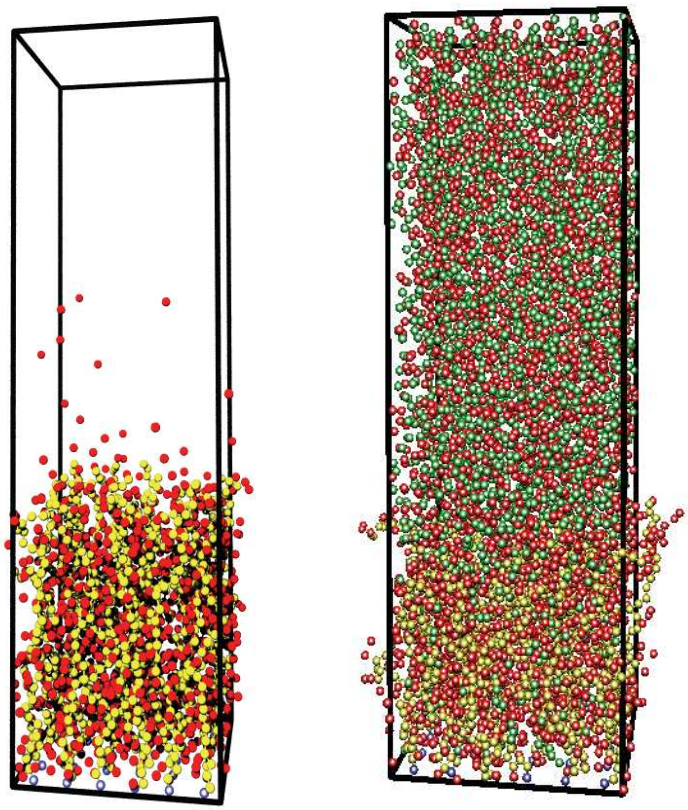


Figure 2. Snapshots of polyelectrolyte brushes with 36 chains of 30 monomers each (yellow) from MD simulations. The chains are fully charged; Bjerrum length is set $l_B = \sigma$. Left-hand side: saltless, counterions are colored red; right-hand side: with additional salt, coions are colored green, counterions red. The snapshots out of equilibrium trajectories have been represented by using the visualization program VMD[5] and the rendering program POV-Rays[6].

3 Nonlinear Osmotic Brush Regime

Figure 2 (left-hand side) shows a snapshot from the simulation at electrostatically intermediate coupling strength ($l_B = \sigma$). Note that there are only about 1% of counterions

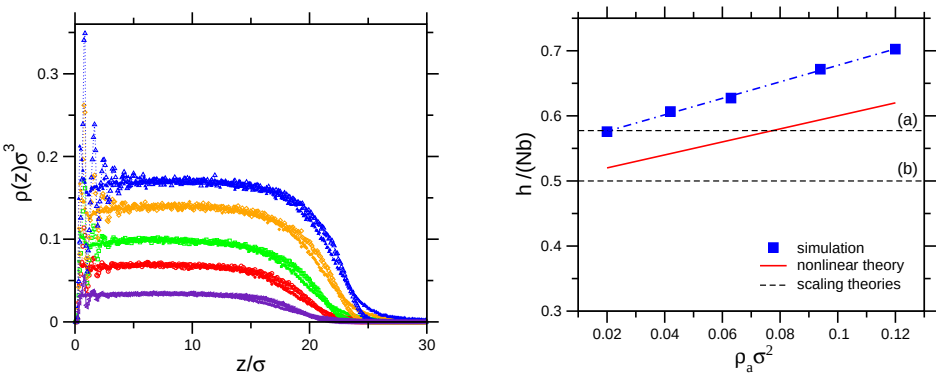


Figure 3. Simulation results of fully charged brushes ($N = 30, l_B = \sigma$). Left-hand side: density profiles of monomers and counterions (see the text) at grafting densities between $0.02\sigma^{-2}$ (bottom) and $0.12\sigma^{-2}$ (top); right-hand side: brush height as a function of grafting density, simulation data and theoretical predictions.

outside the brush, i.e., in a quite reasonable approximation the brush can be considered to be locally electro-neutral. Simulated density profiles of monomers and counterions are plotted for several grafting densities ρ_a) in Fig. 3 (left-hand side). In agreement with the snapshot, both monomers and counterions follow very similar nearly steplike profiles with uniform amplitude inside the brush, which increases with grafting density. Only at the rim of the brush there appear some differences: a depletion of counterions occurs inside and a corresponding tail of the density profile outside the brush. At that point the conclusion is that the brush is in the strong-charging limit where the stretching of the chains is caused by the osmotic pressure of counterions[7]. The average height of end-points of the chains is shown in Fig. 3 (right-hand side). The simulated brush height varies slowly with the grafting density, contrary to the predictions of standard scaling theories[8,9], but in agreement with recent experimental results and in agreement with a scaling theory that incorporates nonlinear elastic and nonlinear osmotic effects[7].

The brush height h in the osmotic regime is given by the balance of the osmotic pressure of counterions and the elastic response due to the stretching of chains. From Fig. 3 (right-hand side) one can see that the chains are stretched up to about 60% of their contour length. Thus their behavior is far beyond the linear regime. But, non-linear elasticity alone does not change the dependence on grafting density. However, the counterion free energy contains entropic contributions that depend on the volume being available for the counterions. Using a free volume approximation very much in the spirit of the van der Waals equation for the liquid-gas transition, the available volume (per chain) $V_0 = h/\rho_a$ is reduced by the self-volume of the chain $\upsilon = Nb\sigma_{\rm eff}^2$. Note that the effective polymer radius $\sigma_{\rm eff}$ takes into account both the monomer and counterion size. Thus the free volume is given by $V = V_0(1-\eta)$ with $\eta = \rho_a\sigma_{\rm eff}^2 Nb/h$ being the degree of close packing in the brush. Balancing the resulting nonlinear entropy of counterions with the high stretching chain elasticity, the equilibrium brush height in the nonlinear osmotic regime becomes[7]

$$h_{\rm NlOsB} = Nb\,\frac{f+\sigma_{\rm eff}^2\rho_a}{1+f}, \qquad (2)$$

where f is the degree of charging. The theoretical line (nonlinear theory) shown in Fig. 3 (right-hand side) is calculated with $\sigma_{\rm eff}^2 = 2\sigma^2$. This choice corresponds to a two-dimensional square-lattice packing of monomers and counterions on two interpenetrating sublattices. The nonlinear prediction given in Eq. 2 qualitatively captures the slow increase of the brush height with grafting density. The deviations from the simulation data may be explained by considering additional effects which go beyond the simple extension of the scaling analysis.

4 Effect of Additional Salt

According to Pincus[8] the brush shrinks with increasing salt concentration, but only as a relatively weak power law $c_s^{-1/3}$. There is some experimental and theoretical work that confirms this prediction, but there are other results that are in contradiction. The aim of our simulation study is to clarify that question.

Figure 2 (left-hand side) shows a snapshot from the simulation at electrostatically intermediate coupling strength ($l_B = \sigma$) and rather high salt concentration ($c_s = 0.11\sigma^{-3}$). In contrast to the saltless case, now the particle distribution looks rather homogeneous over the total height of the simulation box. Because polyelectrolyte counterions and salt counterions are considered to be identical they are subject to an unrestricted exchange. As one can see from the snapshot, salt coions are diffusing into the brush layer. Although it can not be seen directly in snapshots, due to local electroneutrality these coions are escorted by a corresponding number of counterions. The different aspects of the ion distribution inside and outside the brush layer will be discussed below in detail.

The average thickness of the brush is measured by taking the first moment of the monomer density profile. To obtain an universal scaling curve in Fig. 4 (left-hand side) we plot $h(c_{\rm s})/h_0$ vs $bc_{\rm s}/(\rho_{\rm a} f^{1/2})$. However, to rescale the brush height with the theoretical salt-free value h_0 instead of the osmotic brush height we use that of the non-linear osmotic

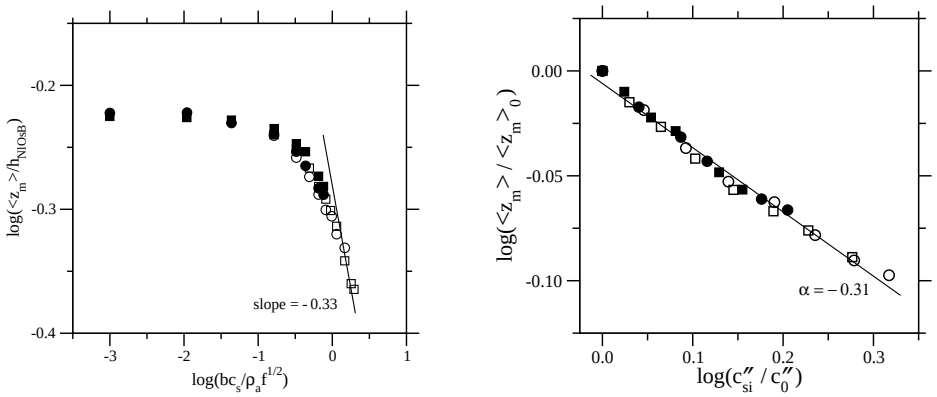


Figure 4. Simulation results of fully charged brushes ($N = 30, l_B = \sigma$) with additional salt. Left-hand side: brush height versus salt concentration; right-hand side: brush height versus ion concentration inside the brush.

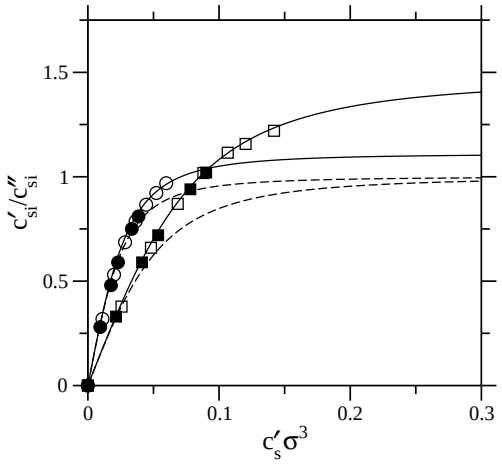


Figure 5. Relation between the ion concentration inside the brush $c''_{\rm si}$ and buffer concentration $c'_{\rm si}$ versus salt concentration $c'_{\rm s}$ for two different grafting densities. Simulation results (symbols) and predictions of original (dashed lines) and modified (solid lines) Donnan approach.

brush given in Eq. (2), where the effective polymer thickness is set again $\sigma^2_{\rm eff} = 2\sigma^2$[10]. Thus, all the data points fall indeed onto a universal curve in a log-log plot, which tends to a slope of zero in the low salt regime indicating the validity of the non-linear osmotic brush relation.

On the other hand, obviously the limit of a salted brush $c_{\rm s} \gg c_{\rm ci}$ where the influence of counterions can be neglected, is hard to reach. Although at the largest salt concentration we consider one observes indeed a slope that is in agreement with the Pincus prediction one has to pay attention to the very few data points in that region. However, a further increase of the total number of charges would enlarge the CPU time beyond a reasonable limit and a reduced size of the simulation box would cause serious finite size effects. Therefore, to account properly for the screening within the brush, the counterion concentration $c_{\rm ci}$ cannot be neglected.

The concentration of small ions inside the brush $c''_{\rm si}$ is obtained by counting the mobile ions within the layer $0 < z < z_{\rm i}$ where $z_{\rm i}$ is the inflection point in the monomer density profile that is used as a measure of the rim of the brush. On a log-log scale, in Fig. 4 (right-hand side), we plot the average brush height $\langle z_{\rm m} \rangle$ versus the ion concentration inside the brush $c''^{10}_{\rm si}$. Both $\langle z_{\rm m} \rangle$ and $c''_{\rm si}$ are rescaled with the corresponding salt-free values $\langle z_{\rm m} \rangle_0$ and c''_0 respectively. The brush height scales with $c''_{\rm si}$ showing an exponent $\alpha \approx -0.31$. This result is in good agreement with the scaling law $h \sim c_{\rm s}^{-1/3}$ predicted by Pincus for the salt dependence of the brush height in the osmotic regime[8]. Note that different symbols in Fig. 4 refer to different grafting densities while open and filled symbols indicate different system sizes. Thus, from Fig. 4 it becomes clear that finite-size effects due to the setting of the box height do not affect the scaling behavior.

To get the relationship between the ion concentration inside the brush $c''_{\rm si}$ and the buffer concentration $c'_{\rm si}$, in Fig. 5 we plot the ratio $c'_{\rm si}/c''_{\rm si}$ versus the salt concentration $c'_{\rm s}$. From

the point of view of the ion distribution perpendicular to the grafting plane a polyelectrolyte brush is very similar to the membrane equilibria problem where the membrane is impermeable to macro-ions but permeable to small ions. Hence one can divide the simulation box into two compartments with the membrane "boundary" located at the rim of the brush that is defined in our model by z_i. Due to the presence of the macro-ions in one compartment similarly charged ions are expelled from this compartment, giving rise to a somewhat non-homogeneous distribution of the small ions as already pointed out by Donnan in 1911[11]. Applying the Donnan approach to the brush system the ratio of the small ions in both compartments becomes

$$\frac{c'_\mathrm{si}}{c''_\mathrm{si}} = \left[1 + \left(\frac{fN\rho_\mathrm{a}}{2z_\mathrm{i}c'_\mathrm{s}}\right)^2\right]^{-1/2}. \tag{3}$$

In Fig. 5, the predictions following from Eq. (3) are given by dashed lines. Obviously the behavior disagrees with the simulation data that do not give a uniform ion concentration in the high-salt limit. We find a surplus of small ions on the polymer-free side that is growing with increasing grafting density, i.e., with enhanced polymer concentration.
Note that the Donnan effect has been evaluated for a system of point-like constituents. While such an approximation is appropriate for dilute solutions it fails for rather dense phases like polymer brushes. Including the polymer self-volume in a free-volume approximation as introduced above the Donnan equilibrium reads[10]

$$\frac{c'_\mathrm{si}}{c''_\mathrm{si}} = \frac{1}{1-\eta}\left[1 + \frac{1}{(1-\eta)^2}\left(\frac{fN\rho_\mathrm{a}}{2z_\mathrm{i}c'_\mathrm{s}}\right)^2\right]^{-1/2}. \tag{4}$$

Using the same σ_eff as above, finally we obtain an almost perfect agreement with the simulation data.

5 Conclusion

Performing extensive molecular dynamics simulations which require the use of massively parallel supercomputers new insight into the behavior of polyelectrolyte brushes could be obtained. These new findings stimulated both the development of theory and the realization of new or improved experiments. Thus numerical simulations gave rise to an increased knowledge about a polymer system that is of high interest from the point of view of both fundamental and applied research.

Acknowledgments

We gratefully acknowledge a grant for the IBM Regatta supercomputer at NIC Jülich, Germany. We thank Axel Arnold for helpful comments on his MMM2D code and Roland Netz for useful discussions.

References

1. M. P. Allen and D. J. Tildesley, *Computer Simulation of Liquids*, Oxford University Press (1987).
2. R. Strebel and R. Sperb, Mol. Simul. **27**, 61–74 (2001).
3. A. Arnold and C. Holm, Comput. Phys. Commun. **148**, 327–348 (2002).
4. W. Gropp, E. Lusk, and A. Skjellum, *Using MPI*, The MIT Press (1994).
5. `http://www.ks.uiuc.edu/Research/vmd/`
6. `http://www.povray.org/`
7. H. Ahrens, S. Förster, C. A. Helm, N. A. Kumar, A. Naji, R. R. Netz, and C. Seidel, *Nonlinear Osmotic Brush Regime: Experiments, Simulations and Scaling Theory*, J. Phys. Chem. B **108**, 16870–16876 (2004).
8. P. Pincus, Macromolecules **24**, , (2912–2919) 1991.
9. O. V. Borisov, T. M. Birshtein, and E. B. Zhulina, J. Phys. II (Paris) **1**, 521–526 (1991).
10. N. A. Kumar and C. Seidel, *Polyelectrolyte Brushes with Added Salt*, Macromolecules **38**, 9341–9350 (2005).
11. F. G. Donnan, Z. Elektrochem. **17**, 572 (1911).